RESEARCH ARTICLE

A novel thermostable aspartic protease from *Talaromyces leycettanus* and its specific autocatalytic activation through an intermediate transition state

Yujie Guo[1], Tao Tu[1], Yaxin Ren[1], Yaru Wang[1], Yingguo Bai[1], Xiaoyun Su[1], Yuan Wang[1], Bin Yao[1], Huoqing Huang[1]*, Huiying Luo[1]*

[1]Key Laboratory for Feed Biotechnology of the Ministry of Agriculture, Feed Research Institute, Chinese Academy of Agricultural Sciences, Beijing 100081, P. R. China

Running title: Insights into a specific auto-activation of pro*Tl*APA1

* Corresponding authors.

E-mail addresses: luohuiying@caas.cn (H. Luo), huanghuoqing@caas.cn (H. Huang).

ABSTRACT

Aspartic proteases exhibit optimum enzyme activity under acidic condition and have been extensively used in food, fermentation and leather industries. In this study, a novel aspartic protease precursor (pro*Tl*APA1) from *Talaromyces leycettanus* was identified and successfully expressed in *Pichia pastoris*. Subsequently, the auto-activation processing of the zymogen pro*Tl*APA1 was studied by SDS-PAGE and N-terminal sequencing, under different processing conditions. *Tl*APA1 shared the highest identity of 70.3 % with the aspartic endopeptidase from *Byssochlamys spectabilis* (GAD91729) and was classified into a new subgroup of the aspartic protease A1 family, based on evolutionary analysis. Mature *Tl*APA1 protein displayed an optimal activity at 60 °C and remained stable at temperatures of 55 °C and below, indicating the thermostable nature of *Tl*APA1 aspartic protease. During the auto-activation processing of pro*Tl*APA1, a 45 kDa intermediate was identified that divided the processing mechanism into two steps: formation of intermediates, and activation of the mature protein (*Tl*APA1). The former step was completely induced by pH of the buffer, while the latter process depended on protease activity. The discovery of the novel aspartic protease *Tl*APA1 and study of its activation process will contribute to a better understanding of the mechanism of aspartic proteases auto-activation.

IMPORTANCE

The novel aspartic protease *Tl*APA1 was identified from *T. leycettanus* and expressed as a zymogen (pro*Tl*APA1) in *P. pastoris*. Enzymatic characteristics of the

mature protein were studied and the specific pattern of zymogen conversion was described. The auto-activation processing of pro*Tl*APA1 proceeded in two stages and an intermediate was identified in this process. These results describe a new subgroup of aspartic protease A1 family and provide insights into a novel mode of activation processing in aspartic proteases.

KEYWORDS: aspartic protease; *Talaromyces leycettanus*; molecular evulation; autoproteolytic processing;

INTRODUCTION

Proteases (EC 3.4.11-24) make up a large share of the total global industrial enzymes (1). They have extensive applications in the dairy, baking, beverages, brewing, meat and functional food industries (1, 2). On the basis of the optimal pH of hydrolysis, proteases have been grouped into three categories–acidic, neutral, and alkaline proteases. They can also be classified into serine, cysteine, metallo and aspartic proteases, depending upon their catalytic residues. Aspartic proteases (EC 3.4.23) have two aspartic residues at their catalytic center, which are vital for hydrolytic cleavage of peptide bonds (3). The activity of aspartic proteases can be specifically inhibited by pepstatin A. Molecular weights of aspartic proteases commonly range between 30 to 50 kDa, while some can weigh up to 55 kDa. Aspartic proteases are generally considered as acidic proteases, because they have isoelectric points of 3.0–4.5 and show optimal activity at pH 3.0–5.0. Most aspartic proteases

have an optimal temperature in the range of 30–50 °C, while some exhibit maximum activity at 55 °C. Most aspartic proteases are also sensitive to high temperatures and show poor thermostability, limiting their applications to mesophilic conditions. Thus, the thermal stability of aspartic proteases has been the subject of attention in many recent studies (4). The discovery of novel thermostable enzymes, especially from extremophiles, is a potential method to tackle the aforesaid problem (2, 5).

Aspartic proteases are wide spread in many organisms–vertebrates, insects, plants, fungi and even viruses have been widely reported as sources of aspartic proteases (6). The production of aspartic proteases from fungi has several advantages including short productive cycle, simple late purification, and low costs (7). Most commercial aspartic proteases used currently in industrial production are derived from filamentous fungi. Aspartic proteases from fungi are mainly categorized into two groups–pepsin-like and rennin-like enzymes (8). The pepsin-like enzymes include aspergillopepsin (9), penicillopepsin (10), trichodermapepsin (11) and rhizopuspepsin (12); while the rennin-like enzymes are mainly produced by *Mucor*, *Rhizomucor* and *Chryphonectria* (3). However, the yield of fungal aspartic proteases by industrial fermentation is usually low. An aspartic protease from *Aspergillus foetidus* was extracellularly produced with a activity of only 63.7 U/mL (13). *Pichia pastoris* is an excellent expression system that has been effectively used to solve the problems of low yield of proteases. Many aspartic proteases have been heterogeneously expressed in *P. pastoris* (14, 15, 16). An aspartic protease from *Rhizomucor miehei* was produced in *P. pastoris* with the activity of 3480.4 U/mL (17).

Typical aspartic proteases are initially synthesized in the form of inactive precursors (zymogens), which protect host cells from proteolysis (6). The functions of the N-terminal pro-segments of aspartic proteases have been studied extensively and include facilitating correct folding, blocking the active site, and stabilizing the protein (18, 19). It is generally accepted that the propeptides are auto-catalytically cleaved at acidic pH (20, 21, 22), and their further processing by other peptidases is important for the activation of aspartic proteases from *Candida parapsilosis* (23). Crystal structures of some aspartic protease zymogens and their activation intermediates have been reported (20, 21, 24, 25, 26), which contribute to the understanding of propeptide interactions with catalytic proteins. Current studies on zymogen activation have mainly concentrated on aspartic proteases associated with diseases (22, 27), yet little is known about this process among aspartic proteases from fungi. There is evidence that the predicted zymogens vary in length depending on each fungus, suggesting their unique activation processes (6). Therefore, studying the activation processing of fungal aspartic proteases is of great significance to understand the mode of activation of the whole family.

Given the importance of novel and thermostable aspartic proteases in industrial processes, a gene coding for a novel thermostable aspartic protease, *Tlapa1*, was found and cloned from the thermophilic filamentous fungus *Talaromyces leycettanus*. Phylogenetic analysis indicated that *Tl*APA1 belonged to a new subgroup of aspartic proteases A1 family. Moreover, *Tl*APA1 has been previously expressed in *P. pastoris* in its zymogen form and its auto-activation has been studied in detail. The

auto-activation process of *Tl*APA1 was affected by pH and enzymatic activity, and occurred in two stages distinguished by the presence of a processing intermediate. The mature proteases with activity were subsequently purified and characterized biochemically. In this study, a novel thermostable aspartic protease was discovered and synthesized as a zymogen in *P. pastoris*, and its autocatalytic activation was studied.

RESULTS

Gene cloning and sequence analysis. The gene encoding a novel aspartic protease zymogen was identified from the genome of *Talaromyces leycettanus* and named as pro*Tlapa1*. The DNA sequence (MK108371 in the GenBank database) had 1275 bp consisting of 3 introns and 4 exons. pro*Tlapa1* encode a polypeptide of 424 amino acids including a putative signal peptide of 19 residues and a propeptide of 61 residues at the N-terminus. The molecular mass and p*I* value were estimatedto be 42.5 kDa and 4.7, respectively. Three *N*-glycosylation sites (N144, N253 and N357) were predicted using the NetNGlyc 1.0 Server. The deduced amino acid sequence of pro*Tlapa1* shared the highest identity of 70.3 % with the aspergillopepsin A-like aspartic endopeptidase from *Byssochlamys spectabilis* (GAD91729, 28), and of only 41.4% with a functionally characterized aspergillopepsin-1 from *Aspergillus oryzae* RIB40 (Q06902, 29). Among aspartic proteases with determined three-dimensional structures, pro*Tlapa1* (residues 86 to 405) showed the highest identity (41.7%) with the corresponding domain of the mature aspartic protease (PDB 1IZD) from *Aspergillus oryzae* (30).

Phylogenetic analysis of *Tl*APA1. The results of BLASTP analysis showed that *Tl*APA1 belonged to the A1 family of aspartic proteases. However, this family of proteases comprises of many subgroups with complex evolutionary relationships. To obtain a clear evolutionary relationship between *Tl*APA1 and other homologs of the A1 family, a phylogenetic analysis based on the amino acid sequence alignment was performed using MEGA 7.0. These results indicated that aspartic proteases from

different microorganism were separated from each other in the evolutionary tree (Fig. 1). Seven subgroups that had been reported in previous studies emerged in the process of evolution in the following order: aspergillopepsin, penicillopepsin, trichoderpepsin, podosporapepsin, endothiapepsin, rhizopuspepsin, and murcorpepsin subgroups. However, *Tl*APA1 did not belong to any of these subgroups. *Tl*APA1 along with Q4WZS3 from *Aspergillus fumigates* belonged to a new clade in the evolutionary tree (Fig. 1). This clade emerged after the formation of the rhizopuspepsin subgroup in the evolutionary tree. The evolutionary position of *Tl*APA1 suggested that *Tl*APA1 might have unique characteristics distinct from other aspartic peptidases.

Heterologous expression and purification of proenzyme. The zymogen pro*Tl*APA1, consisting of the N-terminal propeptide and the mature domain, was expressed in *P. pastoris* GS115. Expression of the recombinant protein was confirmed by electrophoresis. As shown by SDS-PAGE (Fig. 2), a specific protein band corresponding to a molecular mass of approximately 53 kDa was obtained, which was higher than the calculated value (45 kDa) of pro*Tl*APA1. Upon treating the samples with Endo H, the target band appeared at approximately 45 kDa. The first five residues of purified pro*Tl*APA1 were V-P-A-P-S, as identified by N-terminal amino acid sequence analysis. These results indicated that *Tl*APA1 was produced in the form of a zymogen in *P. pastoris* GS115.

Process of auto-activation. The inactive precursors of aspartic proteases were usually auto-catalytically activated under acidic conditions. In this study, the processing of the zymogen conversion was determined by SDS-PAGE and N-terminal

amino acid sequencing. As shown in Fig. 3, the activation process had been already initiated at 0 min of incubation at a room temperature (about 25 °C), indicating the rapidity of the process, potentially due to disintegration of zymogens in the reaction whose pH had been adjusted to 3.5 before incubation. The appearance of two new bands was accompanied by the weakening of the zymogen band (50 kDa) before 30 min of incubation (Fig. 3). The molecular weights of the two new products were 45 kDa and 40 kDa, and their first 5 residues were identified as L-D-F-E-P and V-A-Q-P-A, respectively. After 90 min of incubation at room temperature at pH 3.5, the pro*Tl*APA1 was completely converted to a 40 kDa band (Fig. 3). We suspected that the 45 kDa product was an intermediate in the conversion process of pro*Tl*APA1 to mature *Tl*APA1, and the processing sites on this 45 kDa product were confirmed by N-terminal sequencing. The above results indicated that the precursors pro*Tl*APA1 could be processed into its mature form in an intermolecular manner, and two processing sites (L67-L68, D85-V86) of pro*Tl*APA1 auto-activation were identified.

Effects of proteolytic activity on auto-activation processing. As previous studies have illustrated, processing induced auto-activation was related to its own proteolytic activity. Pepstatin A is a specific inhibitor of aspartic protease, which can effectively inhibit its protease activity. Hence, the effect of pepstatin A on the zymogen conversion of *Tl*APA1 was examined at a concentration of 5 μM of pepstatin A. Electrophoretic analyses revealed that upon pepstatin A treatment, the apparent molecular mass of the pro*Tl*APA1 decreased from 50 to 45 kDa (Fig. 4). The first 5 amino acid residues of processed proteins (45 kDa) were determined as L-D-F-E-P,

which were identical to the cleavage intermediate of *Tl*APA1. This result indicated that auto-processing intermediates (45 kDa products) were produced in the presence of pepstatin A. However, the mature protein (40 kDa) was not obtained even upon prolonged the incubation time up to 3 h. This demonstrated that the activation process from intermediates to mature proteins was inhibited by pepstatin A. Hence, we concluded that the activation process from intermediates to mature protein was accompanied by proteolytic processing. We also studied the effect of catalytic residue of *Tl*APA1 on zymogen conversion by replacing the catalytic Asp103 residue with Asn. This showed that although the catalytic mutant did not prevent processing of the precursor into the 45 kDa intermediate, it terminated the auto-activation of pro*Tl*APA1 in the intermediate stage (data not shown). The above results show that the two phases of the auto-activation process of pro*Tl*APA1 were independent of each other, and the activity of aspartic proteases had greater effect on the latter stage rather than on the former.

Effect of pH on auto-activation processing. The auto-activation processing of aspartic proteases is often triggered by low pH. To determine the optimum pH of zymogen conversion, this processing was executed in range of pH 3.0–6.0, and the proteolytic activities of treated samples were detected using casein (1%, w/v) as a substrate, during the processing of the aspartic protease zymogen. During prolonged incubation at pH 3.0, the proteolytic activities were increased and the enzyme activity peaked after 60 min (Fig. 5A). We speculated that the precursor was almost completely processed after 60 min of incubation at pH 3.0, which was confirmed by

196 SDS-PAGE (Fig. 5B, pH 3.0). The processing induced auto-activation at pH 4.0 and
197 pH 3.0 were comparable, although complete activation at pH 4.0 required longer
198 incubation time (about 90 min). As shown in Fig. 5A, the increasing of proteolytic
199 activities was absent at pH 6.0, and no differences in protein bands were observed
200 (Fig. 5B, pH 6.0). This indicated that zymogen pro*Tl*APA1 was not converted at pH
201 6.0. Interestingly, the precursor band was cleaved at pH 5.0 (Fig. 5B), although the
202 final activity was dramatically lower than at pH 3.0 and pH 4.0. In order to understand
203 the reason for the lowered activity at pH 5.0, the N-terminal amino acid sequences of
204 mature proteins at pH 3.0 and pH 5.0 were determined, and found to be V-A-Q-P-A
205 and A-V-Q-G-G. This demonstrated that two different mature proteins were
206 generated– *Tl*APA1 at pH 3.0 and M2-*Tl*APA1 at pH 5.0, however, the mature protein
207 M2-*Tl*APA1 was inactive. In conclusion, precursors of aspartic proteases could be
208 activated at the range of pH 3.0–4.0, while auto-activation occurred most efficiently at
209 pH 3.0, which is closest to the optimum pH of mature aspartic protease.

210 **Biochemical characterization of *Tl*APA1.** The enzymatic characteristics of mature
211 aspartic proteases *Tl*APA1 and M2-*Tl*APA1 were assessed using casein (1%, w/v) as a
212 substrate. *Tl*APA1 showed the highest activity at pH 3.5 (Fig. 6A), similar to that that
213 seen in most fungal aspartic proteases. As shown in Fig. 6B, *Tl*APA1 had an optimal
214 temperature of 60 °C, which was higher than aspartic proteases obtained from most
215 other fungi. We further measured stabilities of aspartic protease *Tl*APA1 under
216 different pH and temperature conditions. *Tl*APA1 retained greater than 80 % of its
217 initial activity after 60 min of incubation at 37 °C over a range of pH 2.0–6.0 (Fig.

6C). The stability at acidic pH makes *Tl*APA1 favorable for applications in food, beverages, and brewing industries. Fig. 6D shows that *Tl*APA1 was extremely stable below 55°C, retaining almost all of its initial activity after 1 h of incubation. At higher temperatures, half-life of *Tl*APA1 was 30 min at 60 °C and 5 min at 65 °C. The thermostability of *Tl*APA1 was higher than that of highly homologous aspartic proteases from other fungi. M2-*Tl*APA1 activity was not detected at any of the aforementioned temperature and pH conditions. Purified recombinant *Tl*APA1 had a specific activity of 2187.4 ± 67.3 $U \cdot mg^{-1}$, while the K_m, V_{max}, k_{cat}, and k_{cat}/K_m values were determined as 1.9 $mg \cdot mL^{-1}$, 2,321 $\mu moL \cdot min^{-1} \cdot mg^{-1}$, 1,410 s^{-1} and 723.5 $mL \cdot s^{-1} \cdot mg^{-1}$, respectively.

DISCUSSION

Novel enzymes with unique characteristics such as pH adaption, thermostability and tolerance to metal ions are in valuable for research and industrial purposes (31). Extremophiles are excellent sources of novel enzymes that can retain their integrity and function under extreme reaction conditions (32). *Talaromyces leycettanus* JCM12802, a thermotolerant fungus, that has an optimal growth temperature of 42 °C, is the source of various thermostable hydrolases including *β*-mannanase (33), xylanase (34), *β*-glucanase (35), and *α*-Amylase (36). In this study, a novel aspartic protease precursor comprising of 424 amino acid residues was identified in *Talaromyces leycettanus* and was determined to be a member of the A1 family of aspartic proteases.

A1 family, the most well studied one of the 16 families of aspartic proteases, is

241 further subdivided into 5 super families (AA, AC, AD, AE, and AF) (37). Pfam
242 protein family prediction indicated that *Tl*APA1 belonged to the A1 family, one that
243 contains many biochemically-characterized enzymes including pepsin, chymosin,
244 rennin, and cathepsin D (37, 38). When full sequences of the A1 family proteins were
245 used for phylogenetic analysis, the phylogenetic tree indicated *Tl*APA1 as a sister to
246 an uncharacterized aspartic protease Q4WZS3 from *Aspergillus fumigates*, whose
247 clade has not yet been discovered (Fig. 1). Phylogenetic analysis is able to provide
248 deeper insights into the evolution of a new clade. The phylogenetic tree showed that
249 *Tl*APA1 largely differed with other homologs in terms of the amino acid sequence,
250 indicating that *Tl*APA1 potentially had distinct enzyme characteristics and special
251 applications like the mucorpepsin subgroup, a unique clade in the evolutionary
252 process and an important class of proteases, widely used as milk coagulating agents
253 (39). The evolution of A1 family has been well studied, which has contributed to an
254 indepth understanding of fungal aspartic protease evolution (40). Fungal aspartic
255 proteases have undergone large sequence diversification leading to their evolutionary
256 complexity (37). To further investigate the evolutionary position of *Tl*APA1 among
257 subgroups of A1 family, a phylogenetic analysis was performed and an evolutionary
258 tree was constructed (Fig 1). Our analysis suggested *Tl*APA1 as a potential
259 evolutionary intermediate linking rhizopuspepsins and other subgroups.

260 The full amino acid sequence of secreted aspartic proteases contains a propeptide
261 region followed by a mature protein (6). The pro*Tl*APA1 zymogen was composed of
262 an N-terminal propeptide of 61 residues, and a mature domain of 339 residues. Our

263 results demonstrated that pro*Tl*APA1 could be processed auto-catalytically into the
264 mature aspartic protease under acidic conditions, consistent with other homologs (41).
265 However, the N-terminal propeptide of pro*Tl*APA1 precursor was processed
266 auto-catalytically in two phases. Firstly, precursors were processed into intermediates
267 driven by pH-dependent structural changes that were not affected by a specific
268 inhibitor or the D103N mutation. Secondly, the process that turned intermediates into
269 mature enzymes was auto-catalyzed by enzymes; that could be stalled in the presence
270 of a specific inhibitor or mutation of active residues. We further studied the
271 conversion processing of pro*Tl*APA1 at different pH conditions and determined that
272 the optimum pH of conversion was similar to that of its peak activity. Interestingly,
273 when we activated the zymogens at pH 5.0, a minor mature protein band was
274 generated in SDS-PAGE. This auto-processing site (S98-A99) was also confirmed by
275 N-terminal sequencing, and was located 13 residues downstream of the first mature
276 site. However, the mature products at pH 5.0 had no proteolytic activity (Fig 7). The
277 large differences in the processing of pro*Tl*APA1 compared to other homologs could
278 arise from the N-terminal propeptide of *Tl*APA1 precursor (Fig.S1). The N-terminal
279 propeptide of *Tl*APA1 precursor showed low sequence identity (< 30%) to other
280 known aspartic proteases. The N-terminal propeptide of *Tl*APA1 precursor possessed
281 an additional 61 residues with a greater abundance of arginine residues, compared to
282 other homologs (Fig.S1). We thus speculated that the sequence peculiarity of
283 N-terminal pro-segment lead to the special auto-activation processing of the *Tl*APA1
284 precursor.

Generally, aspartic proteases exhibit activities and stabilities in the acidic pH range (20). Purified *Tl*APA1 showed a peak activity at pH 3.5, and was stable over the pH range of 3.0 to 6.0. These characteristics were similar to the homologs from other fungi, including *Monascus pilosus* (42), *Trichoderma asperellum* (14), and *A. foetidus* (13). The acidic adaptation of *Tl*APA1 makes it a promising candidate in many industries including cheese manufacturing, juice clarification, and leather softening. *Tl*APA1 also hydrolyzed proteins at higher temperatures. Its optimal activity was recorded at 60 °C and greater than 80% of the maximal activity was remained at 65 °C. The temperature optimum of *Tl*APA1 is higher than most reported homologs (Table 2). *Tl*APA1 retains greater than 80 % of its original activity after incubation at 55 °C for 30 min, indicating superior thermostability of *Tl*APA1 compared to most other aspartic proteases that are commonly stable at 45°C and below (Table 2). The thermostability of *Tl*APA1 is a favorable characteristic its potential application in many areas. For example, during proteolysis, most substrate proteins are resistant to proteases because of their structural stability at moderate temperatures. At higher temperatures, substrate proteins become unfold and their cleavage sites become exposed and accessible to the catalytic enzyme. This suggests more efficient hydrolysis of *Tl*APA1 substrates at high temperatures, due to the thermostable nature of *Tl*APA1.

In summary, a novel aspartic protease, *Tl*APA1, was identified, that belonged to a new clade in the phylogenetic tree. The sequence analysis of the propeptide region showed that pro*Tl*APA1 could have a unique mechanism of auto-activation processing.

307 The results indicated that there are two steps in the processing of auto-activation, and
308 a 45 kDa intermediate was confirmed. Moreover, the characteristics of mature protein
309 *Tl*APA1 demonstrated that it is excellent in terms of specific activity and
310 thermostability.

MATERIALS AND METHODS

Strains, vectors and substrates. The gene donor strain of *Talaromyces leycettanus* JCM12802 was purchased from Japan Collection of Microorganisms RIKEN BioResource Center. *Escherichia coli* Trans1-T1 (TransGen) was used for gene cloning and sequencing. Target gene was expressed in *P. pastoris* GS115 (Invitrogen). Cloning and expression vectors used were pEASy-T3 (TransGen, Beijing, China) and pPIC9 (Invitrogen, Carlsbad, CA), respectively. Casein sodium salt from bovine milk (C8654, Sigma-Aldrich, St. Louis, MO) was used as a substrate, and other chemicals of analytical grade were commercially available.

Cloning of aspartic protease *Tlapa1* gene. *Talaromyces leycettanus* was cultivated as described previously (36). DNA and total RNA were extracted from the mycelia of *T. leycettanus* JCM12802 after 3 day of growth at 42 °C, and the cDNA was prepared according to the manufacturer's instructions (TOYOBO, Osaka, Japan). The *Tlapa1* gene was amplified from DNA and cDNA of *Talaromyces leycettanus*, respectively, by polymerase chain reaction (PCR) method. The primer pairs used in this study are listed in Table 1. Finally, the PCR products were cloned into the pEASY-T3 and sequenced.

Bioinformatic analysis of *Tlapa1* gene. The sequence results were assembled using DNA Star 7.1 software. The amino acid sequences obtained by the Vector NTI Advance 10.0 software (Invitrogen) were searched with BLASTp programs (http://www.ncbi.nlm.nih.gov/BLAST/) to analyze the homologous sequences. The signal peptide sequence of *Tl*APA1 was predicted with SignalP

(http://www.cbs.dtu.dk/services/SignalP/). The potential *N*-glycosylation sites were predicted using NetNGlyc 1.0 Server (http://www.cbs.dtu.dk/services/NetNGlyc/). Alignment of multiple protein sequences was accomplished using Clustal W software (http://www.clustal.org/) and rendered using the ESPript 3.0 program (http://espript.ibcp.fr/ESPript/cgi-bin/ESPriptcgi).

Phylogenetic analysis. The full amino acid sequence of *Tl*APA1 was used as the query sequence in BLASTp searches in NCBI (http://blast.ncbi.nlm.nih.gov/Blast.cgi). In total, 22 sequences of A1 family aspartic proteases were obtained. Multiple sequence alignments of *Tl*APA1 with other representative aspartic proteases enzymes, characterized enzymes, and enzymes with determined three-dimensional (3D) structures, were performed as described previously (37). Sequence information for the A1 family of aspartic proteases was obtained from the MEROPS database (https://www.ebi.ac.uk/merops/cgi-bin/family_index?type=P#A). Phylogenetic analyses of *Tl*APA1 and A1 family of aspartic proteases were performed as described in previous studies (37). The distance matrix for nucleotides was calculated by Kimura's two-parameter model. The phylogenetic tree was constructed with the neighbor-joining method using MEGA 7.0 and assessed using 1,000 bootstrap replications (46).

Expression and purification of zymogens. Recombinant proteins were expressed in *P. pastoris* GS115, as described previously (36). Briefly, the gene fragment coding for the zymogen (pro*Tl*APA1) without the signal peptide was amplified using PCR method. PCR products were digested with *Eco*RI and *Not*I and ligated into the pPIC9

plasmid using T4 DNA ligase (New England Laboratory). The recombinant plasmid pPIC9-pro*Tlapa1*, linearized by *Bgl*II, was transformed into *P. pastoris* GS115 competent cells by electroporation. Positive transformants were screened based on the transparent zone on skim milk plates as described below. The transformants showing the largest transparent zones were inoculated into 30 mL YPD and incubated at 30 °C. The seed medium containing the positive transformant was inoculated into 1 L conical flasks containing 300 mL of BMGY for fermentation. Conical flasks containing 200 mL of BMMY and 0.5% (v/v) methanol were prepared.

The cells were harvested by centrifugation for 10 min at 12,000*g*, and resuspended in BMMY medium and for next subsequent fermentation at 30 °C. Methanol was added every 24 h to obtain a final concentration of 0.5% (v/v). After 48h of cultivation, cell-free cultures were centrifugated at 12,000 rpm, 4 °C for 10 min and fermentation broth was collected. The crude pro-enzymes were concentrated using an ultrafiltration membrane with a molecular weight cut-off of 10 kDa (Vivascience, Hannover, Germany). A HiTrap Q Sepharose XL 5 mL FPLC column (GE Healthcare, Sweden) was used for purification. Protein binding and equilibration was performed using buffer A (10 mM sodium phosphate, pH 6.0), and a linear gradient of NaCl (0–1.0 M) was used to elute the proteins.

Activation of purified zymogen pro*Tl*APA1. To determine processing of zymogen conversion, pH of the pro*Tl*APA1 samples were adjusted to 3.0 using 0.5 M lactic acid-sodium lactate buffer. pro*Tl*APA1 was auto-catalytically activated at 37 °C for 0, 15, 30, 45, 60, 75, and 90 min, respectively. Processed polypeptides were detected by

377 SDS-PAGE and N-terminal sequencing. To study the effect of pepstatin A on the
378 zymogen conversion of pro*Tl*APA1, 5 μM pepstatin A was added into the conversion
379 system before he auto-catalytic processing and incubated at 37 °C for 15, 30, 45, and
380 60 min, respectively. Zymogen conversion systems were subjected to sodium dodecyl
381 sulfate-polyacrylamide gel electrophoresis (SDS-PAGE) analysis. Samples without
382 pepstatin A were also treated similarly, as a control group. To determine the optimum
383 pH of zymogen conversion, the pH of the pro*Tl*APA1 samples were adjusted to 2.0,
384 3.0, 4.0, 5.0, and 6.0 using 0.5 M lactic acid-sodium lactate buffer. The samples at
385 different pH conditions were incubated at 37 °C, and the proteolytic activities were
386 analyzed with casein (1%, w/v) at different incubation times. Finally, the samples
387 were analyzed using SDS-PAGE.

388 **Enzyme activity assay.** The activity of aspartic proteases was assayed in a 1000 μl
389 reaction mixture containing 500 μl of 1 % (w/v) casein sodium salt and 500 μl
390 enzyme sample in buffer at pH 3.0. After incubation at 60 °C for 10 min, 1000 μl of
391 40 % (w/v) trichloroacetic acid (TCA) was added to terminate the reaction. 500 μL of
392 the supernatant was obtained from the mixture using centrifugation after 12,000*g* for
393 3 min. 2.5 mL of 0.4 M sodium carbonate and 500 μL Folin-phenol was added into
394 supernatant in turn before incubating at 40 °C for 20 min. The amount of released
395 tyrosine was measured at 680 nm. One unit of proteolytic activity was defined as the
396 amount of enzyme that released 1 μmol of tyrosine equivalent per minute under the
397 conditions described above (pH 3.5, 60 °C and 10 min).

398 **Properties of recombinant aspartic protease *Tl*APA1.** Optimal conditions for

399 purified *Tl*APA1 activity were measured in lactic acid-sodium lactate buffer under the
400 following conditions– temperatures ranging from 30 °C to 80 °C (at a constant pH
401 3.5); and pH ranging from 2.0 to 4.5 (at a constant temperature of 60 °C).
402 Thermostability and pH stability of *Tl*APA1 were assessed by preincubating the
403 purified enzyme for 1 h in lactic acid-sodium lactate buffer under varying temperature
404 conditions: 55 °C, 60 °C and 65 °C (at constant pH of 3.5); or varying pH conditions:
405 pH 2.0–11.0 (at constant temperature of 37 °C), respectively, and then determining the
406 residual enzyme activity.

407 The proteolytic activities of *Tl*APA1 were measured under standard conditions
408 (pH 3.5, 60 °C, 10 min) with 0.5–10 mg/mL casein sodium salt, and the constants
409 were determined by linear regression fitting using GraphPad Prism version 7.01. All
410 experiments were performed in three biological and technical replicates.

411 **N-terminal Sequencing.** Purified proteins were separated by SDS-PAGE and electro
412 transfered onto a polyvinylidene difluoride (PVDF) membrane. Stained with
413 Coomassie Brilliant Blue R-250, the target protein bands were excised and subjected
414 to N-terminal amino acid sequence analysis using a PPSQ-33 automatic sequence
415 analysis system (Shimadzu, Kyoto, Japan).

416 **ACKNOWLEDGEMENTS**

417 This work was supported by the National Key Research and Development
418 Program of China (2016YFD0501409-02), the Fundamental Research Funds for
419 Central Non-profit Scientific Institution (Y2017JC31), and the China Modern
420 Agriculture Research System (CARS-41).

REFERENCE

1. Raveendran S, Parameswaran B, Ummalyma SB, Abraham A, Mathew AK, Madhavan A, Rebello S, Pandey, A. 2018. Applications of microbial enzymes in food industry. Food Technol Biotechnol 56:16–30.
2. Zhang Y, He S, Simpson BK. 2018. Enzymes in food bioprocessing–novel food enzymes, applications, and related techniques. Curr Opin in Food Sci 19:30–35.
3. Yegin S, Fernandez-Lahore M, Salgado AJG, Guvenc U, Goksungur Y, and Tari C. 2011. Aspartic proteinases from *Mucor* spp. in cheese manufacturing. Appl Microbiol Biotechnol 89:949–960,
4. Silva RR, Suoto TB, Oliveira TB, Oliveira LCG, Karcher D, Juliano MA, Juliano L Oliveira AHC, Rodrigues A, Rosa, JC. 2016. Evaluation of the catalytic specificity, biochemical properties, and milk clotting abilities of an aspartic peptidase from *Rhizomucor miehei*. J Ind Microbiol Biotechnol 43:1059–1069.
5. Kangwa M, Salgado JAG, Fernandez-Lahore, HM. 2018. Identification and characterization of N-glycosylation site on a *Mucor circinelloides* aspartic protease expressed in *Pichia pastoris*: effect on secretion, activity and thermo-stability. AMB Express 8:157–170.
6. Mandujano-González V, Villa-Tanaca L, Anducho-Reyes MA, Mercado-Flores, Y. 2016. Secreted fungal aspartic proteases: A review. Rev Iberoam Micol 33:76–82.
7. Souza PM, Bittencourt MLD, Caprara CC, Freitas M, Almeida RPC, Silveira D, Fonseca YM, Ferreira EX, Pessoa A, Magalhaes, PO. 2015. A biotechnology perspective of fungal proteases. Braz J Microbiol 46:337–346.

443 8. Rao MB, Tanksale AM, Ghatge MS, Deshpande VV. 1998. Molecular and
444 biotechnological aspects of microbial proteases. Microbiol Mol Biol Rev
445 62:597–635.
446 9. Vishwanatha KS, Rao AGA, Singh SA. 2009. Characterisation of acid protease
447 expressed from *Aspergillus oryzae* MTCC 5341. Food Chem 114:402–407.
448 10. Fraser ME, Strynadka NC, Bartlett PA, Hanson JE, James MN. 1992.
449 Crystallographic analysis of transition-statemimics bound to penicillopepsin:
450 phosphorus-containing peptide analogues. Biochemistry 31:5201–5214.
451 11. Nascimento AS, Krauchenco S, Golubev AM, Gustchina A, Wlodawer A,
452 Polikarpov I. 2008. Statistical coupling analysis of aspartic proteinases based on
453 crystal structures of the *Trichoderma reesei* enzyme and its complex with
454 pepstatin A. J Mol Biol 382:763-778.
455 12. Kumar S, Sharma NS, Saharan MR, Singh R. 2005. Extracellular acid protease
456 from *Rhizopus oryzae*: purification and characterization. Process Biochem
457 40:1701–1705.
458 13. Souza PMD, Werneck G, Aliakbarian B, Siqueira F, Ferreira FEX, Perego P,
459 Converti A, Magalhaes PO, Junior AP. 2017. Production, purification and
460 characterization of an aspartic protease from *Aspergillus foetidus*. Food Chem
461 Toxicol 109:1103–1110.
462 14. Yang X, Cong H, Song J, Zhang J. 2013. Heterologous expression of an aspartic
463 protease gene from biocontrol fungus *Trichoderma asperellum* in *Pichia pastoris*.
464 World J Microbiol Biotechnol 29:2087–2094.

15. Yegin S, Fernandez-Lahore M. 2013. A thermostable aspartic proteinase from *Mucor mucedo* DSM 809: gene identification, cloning, and functional expression in *Pichia pastoris*. Mol Biotechnol 54:661–672.
16. Gama Salgado JA, Kangwa M, Fernandez-Lahore M. 2013. Cloning and expression of an active aspartic proteinase from *Mucor circinelloides* in *Pichia pastoris*. BMC Microbiol 13:250–260.
17. Sun Q, Chen F, Geng F, Luo Y, Gong S, Jiang Z. 2018. A novel aspartic protease from *Rhizomucor miehei* expressed in *Pichia pastoris* and its application on meat tenderization and preparation of turtle peptides. Food Chem 245:570–577.
18. Koelsch G, Mareš M, Metcalf P, Fusek, M. 1994. Multiple functions of pro-parts of aspartic proteinase zymogens. FEBS Lett 343:6–10.
19. Horimoto Y, Dee DR, Yada RY. 2009. Multifunctional aspartic peptidase prosegments, N Biotechnol 25:318–324.
20. Richter C, Tanaka T, Yada RY. 1998. Mechanism of activation of the gastric aspartic proteinases: pepsinogen, progastricsin and prochymosin. Biochem J 335:481–490.
21. Khan AR, Khazanovich-Bernstein N, Bergmann EM, James MNG. 1999. Structural aspects of activation pathways of aspartic protease zymogens and viral 3C protease precursors. Proc Natl Acad Sci USA 96:10968–10975.
22. Dunn BM. 2002. Structure and mechanism of the pepsin-like family of aspartic peptidases. Chem Rev 102:4431–4458.
23. Dostal J, Dlouha H, Malon P, Pichova I, Hruskova-Heidingsfeldova O. 2005. The

precursor of secreted aspartic proteinase sapp1p from *Candida parapsilosis* can be activated both autocatalytically and by a membrane-bound processing proteinase. Biol Chem 386:791–799.

24. Morales R, Watier Y, Bocskei Z. 2012. Human prorenins tructuresheds light on a novel mechanism of its autoinhibition and on its non-proteolytic activation by the (pro)renin receptor. J Mol Biol 421:100–111.
25. Lee AY, Gulnik SV, Erickson JW. 1998. Conformational switching in an aspartic proteinase. Nat Struct Biol 5:866–871.
26. Ostermann N, Gerhartz B, Worpenberg S, Trappe J, Eder J. 2004. Crystal structure of an activation intermediate of cathepsin E. J Mol Biol 342:889–899.
27. Hanova I, Brynda J, Houstecka R, Alam N, Sojka D. Kopacek P, Maresova L, Vondrasek J, Horn M, Schueler-Furman O, Mares M. 2018. Novel structural mechanism of allosteric regulation of aspartic peptidases via an evolutionarily conserved exosite. Cell Chem Biol 25:318–329
28. Oka T, Ekino K, Fukud K, Nomura Y. 2014. Draft Genome Sequence of the Formaldehyde-Resistant Fungus *Byssochlamys spectabilis* No. 5. Genome Announc 2:e01162–13
29. Gomi K, Arikawa K, Kamiya N, Kitamoto K, Kumagai C. 1993. Cloning and nucleotide sequence of the acid protease-encoding gene (pepA) from *Aspergillus oryzae*. Biosci Biotechnol Biochem 57:1095–1100.
30. Kamitori S, Ohtaki A, Ino H, Takeuchi M. 2003. Crystal structures of *Aspergillus oryzae* aspartic proteinase and its complex with an inhibitor pepstatin at 1.9A

509 resolution. J Mol Biol 326:1503–1511.

510 31. Ferrer M, Monica Martinez-Martinez, Bargiela R, Streit WR, Golyshina, OV,
511 Golyshin PN. 2016. Estimating the success of enzyme bioprospecting through
512 metagenomics: current status and future trends. Microb Biotechnol 9:22–34.

513 32. Haki GD, Rakshit SK. 2003. Developments in industrially important
514 thermostable enzymes: a review. Bioresour Technol 89:17–34.

515 33. Wang C, Luo H, Niu C, Shi P, Huang H, Meng K, Bai Y, Wang K, Hua H, Yao B.
516 2015. Biochemical characterization of a thermophilic *β*-mannanase from
517 *Talaromyces leycettanus* JCM12802 with high specific activity. Appl Microbiol
518 Biotechnol 99:1217–1228.

519 34. Wang X, Ma R, Xie X, Liu W, Tu T, Zheng F, You S, Ge J, Xie H, Yao B, Luo H.
520 2017. Thermostability improvement of a *Talaromyces leycettanus* xylanase by
521 rational protein engineering. Sci Rep 7:152–187.

522 35. You S, Tu T, Zhang L, Wang Y, Huang H, Ma R, Shi PJ, Bai YG, Su XY, Lin ZM,
523 Luo HY, Yao B. 2016. Improvement of the thermostability and catalytic
524 efficiency of a highly active *β*-glucanase from *Talaromyces leycettanus*
525 JCM12802 by optimizing residual charge–charge interactions. Biotechnol
526 Biofuels 9:124–135.

527 36. Zhang D, Tu T, Wang Y, Li Y, Luo X, Zheng F, Wang X, Bai Y, Huang H, Su X,
528 Yao B, Zhang T, Luo H. 2017. Improvement of the catalytic performance of a
529 *Talaromyces leycettanus α*-amylase by changing the linker length. J Agric Food
530 Chem 65:5041–5048.

531 37. Revuelta MV, Kan, JALV, Kay J, Have, AT. 2014. Extensive expansion of a1
532 family aspartic proteinases in fungi revealed by evolutionary analyses of 107
533 complete eukaryotic proteomes. Genome Biol Evol 6:1480–1494.
534 38. Rawlings ND, and Barrett AJ. 2013. Introduction: aspartic and glutamic
535 peptidases and their clans, p 3–19. *In* Barrett AJ, Rawlings ND, Woessner JF (ed),
536 Handbook of Proteolytic Enzymes, 3rd ed, vols 2. Elsevier, Amsterdam.
537 39. Yegin S, Dekker P. 2013. Progress in the field of aspartic proteinases in cheese
538 manufacturing: structures, functions, catalytic mechanism, inhibition, and
539 engineering. Dairy Sci Technol 93:565–594.
540 40. Rawlings ND, Barrett AJ, Thomas PD, Huang X, Bateman A, Finn RD. 2018.
541 The *MEROPS* database of proteolytic enzymes, their substrates and inhibitors in
542 2017 and a comparison with peptidases in the PANTHER database. Nucleic Acids
543 Res 46:624–632.
544 41. Richter C, Tanaka T, Yada RY. 1998. Mechanism of activation of the gastric
545 aspartic proteinases: pepsinogen, progastricsin and prochymosin. Biochem J
546 335:481–490.
547 42. Lakshman PLN, Toyokawa Y, Toyama H, Taira T, Yasuda M. 2010. Purification
548 and characterisation of two extracellular acid proteinases from *Monas cuspilosus*.
549 Food Chem 121:1216–1224.
550 43. Rao S, Mizutani O, Hirano T, Masaki K, Iefuji H. 2011. Purification and
551 characterization of a novel aspartic protease from basidiomycetous yeast
552 *Cryptococcus* sp. S-2. J Biosci Bioeng 112:441–446.

553 44. Takenaka S, Umeda M, Senba H, Koyama D, Tanaka K, Yoshida KI, Doi M.
554 2017. Heterologous expression and characterisation of the *Aspergillus* aspartic
555 protease involved in the hydrolysis and decolorisation of red-pigmented proteins.
556 J Sci Food Agric 97:95–101.
557 45. Kumar S, Stecher G, Tamura K. 2016. Mega 7: molecular evolutionary genetics
558 analysis version 7.0 for bigger datasets. Mol Biol Evol 33:1870–1874.

559 **Figure legends**

560 **Fig. 1** Phylogenetic analysis of the subgroups of aspartic proteases A1 family. The
561 amino acid sequences of A1 family were obtained by a BLAST analysis using the
562 *Tl*APA1 protein (GenBank accession number MK108371) as the query sequence. The
563 evolutionary tree was constructed by the neighbor-joining method. The sequences are
564 labeled with their GenBank accession numbers and host fungi. Numbers indicated in
565 the tree branches are the bootstrap values (%) based on 1000 replications. The
566 subgroups of A1 family are classified using gray shadow and names are indicated in
567 over striking. *Tl*APA1 is shown in red which, together with Q4WZS3, belonged to a
568 new unknown clade.

569

570 **Fig. 2** SDS-PAGE analysis of the recombinant pro*Tl*APA1. Lane M, molecular mass
571 standard; Lane 1, crude zymogen pro*Tl*APA1; Lane 2, purified recombinant
572 pro*Tl*APA1; and Lane 3, deglycosylated zymogen pro*Tl*APA1 treated with Endo H.

573

574 **Fig. 3** Analysis of pro*Tl*APA1 auto-activation for 90 min. The time course of
575 processing at room temperature (~20 °C) was analyzed using 12% SDS-PAGE.
576 Pro*Tl*APA1, recombinant precursor without the signal peptide; Int-*Tl*APA1,
577 intermediate produced during auto-activation processing; Mat-*Tl*APA1, mature
578 protein after auto-activation.

579

580 **Fig. 4** Effect of the inhibitor pepstain A on zymogen auto-processing. The

581 auto-activation processing of recombinant zymogens with or without pepstatin A was
582 analyze using SDS-PAGE at the indicated times. M, molecular mass standard; Pro,
583 purified zymogens before auto-activation. The processing time of the auto-activation
584 ranged from 15–60 (min).

585

586 **Fig. 5** Analysis of pro*Tl*APA1 auto-activation at varying pH 3.0–6.0. (a) Proteolytic
587 activities measured at different times with range of pH 3.0–6.0 at 60 °C. (b)
588 SDS-PAGE analysis of auto-activation processing at 37 °C with pH 3.0, 5.0, and 6.0.

589

590 **Fig. 6** Characterization of purified mature enzyme *Tl*APA1. (a) pH-activity profile. (b)
591 Temperature-activity profile. (c) pH-stability profile after 1 h-incubation at 37 °C at
592 different pH values. (d) Temperature-stability profile after incubation at pH 3.0 and
593 different temperatures for various durations.

594

595 **Fig. 7** Schematic representation of the signal peptide, the propeptide region and the
596 mature protein in *Tl*APA1. Pro*Tl*APA1, the recombinant precursor without the signal
597 peptide; Int-*Tl*APA1, the intermediate produced during auto-activation processing;
598 *Tl*APA1, mature protein after auto-activation at pH 3.0; M2-*Tl*APA1, mature protein
599 after auto-activation at pH 5.0.

600

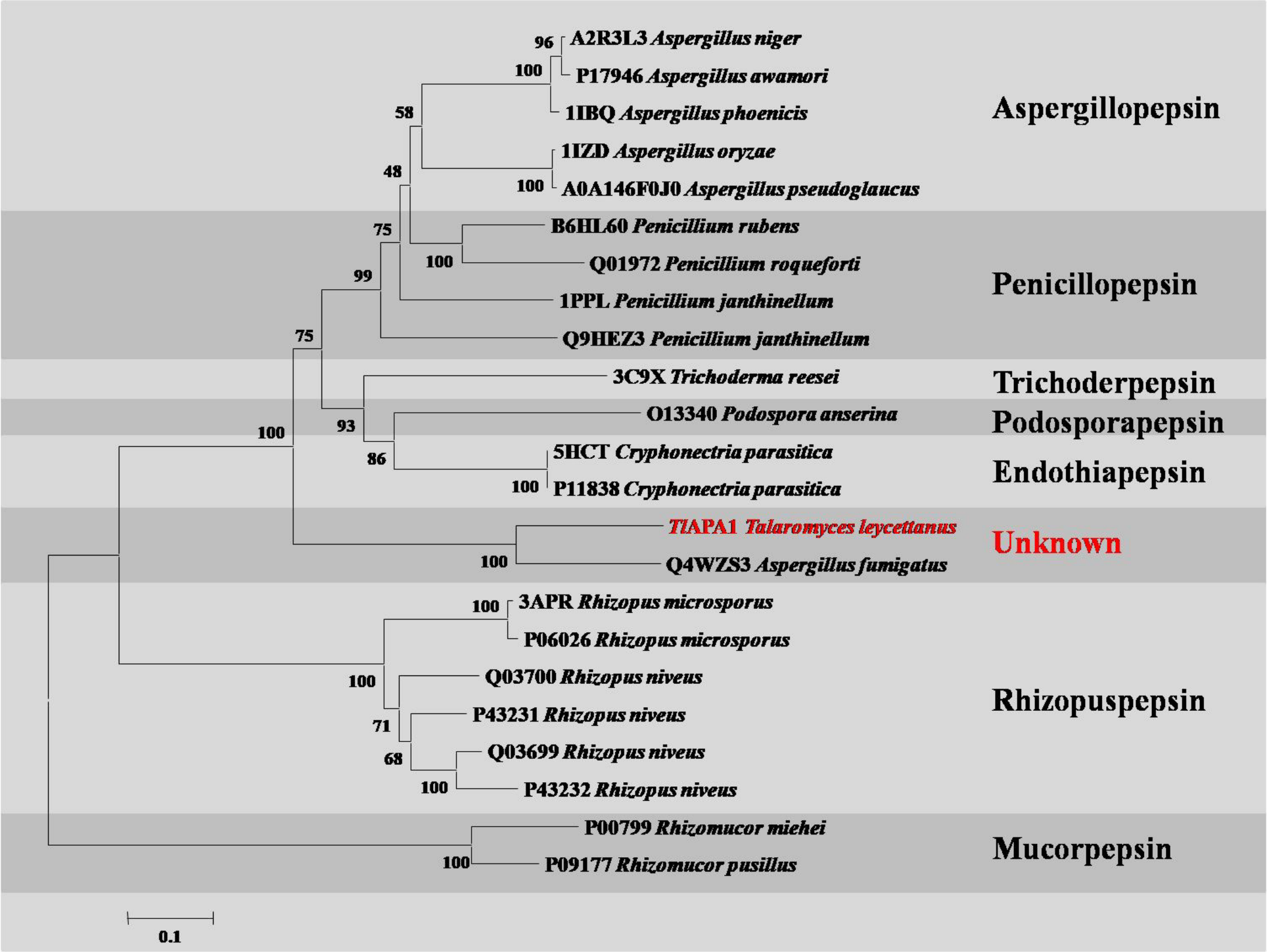
A2R3L3 Aspergillus niger
P17946 Aspergillus awamori
1IBQ Aspergillus phoenicis
1IZD Aspergillus oryzae
A0A146F0J0 Aspergillus pseudoglaucus
B6HL60 Penicillium rubens
Q01972 Penicillium roqueforti
1PPL Penicillium janthinellum
Q9HEZ3 Penicillium janthinellum
3C9X Trichoderma reesei
O13340 Podospora anserina
5HCT Cryphonectria parasitica
P11838 Cryphonectria parasitica
TlAPA1 Talaromyces leycettanus
Q4WZS3 Aspergillus fumigatus
3APR Rhizopus microsporus
P06026 Rhizopus microsporus
Q03700 Rhizopus niveus
P43231 Rhizopus niveus
Q03699 Rhizopus niveus
P43232 Rhizopus niveus
P00799 Rhizomucor miehei
P09177 Rhizomucor pusillus
96
100
58
48
100
75
100
99
75
93
100
86
100
100
100
100
71
68
100
100
0.1
Aspergillopepsin
Penicillopepsin
Trichoderpepsin
Podosporapepsin
Endothiapepsin
Unknown
Rhizopuspepsin
Mucorpepsin

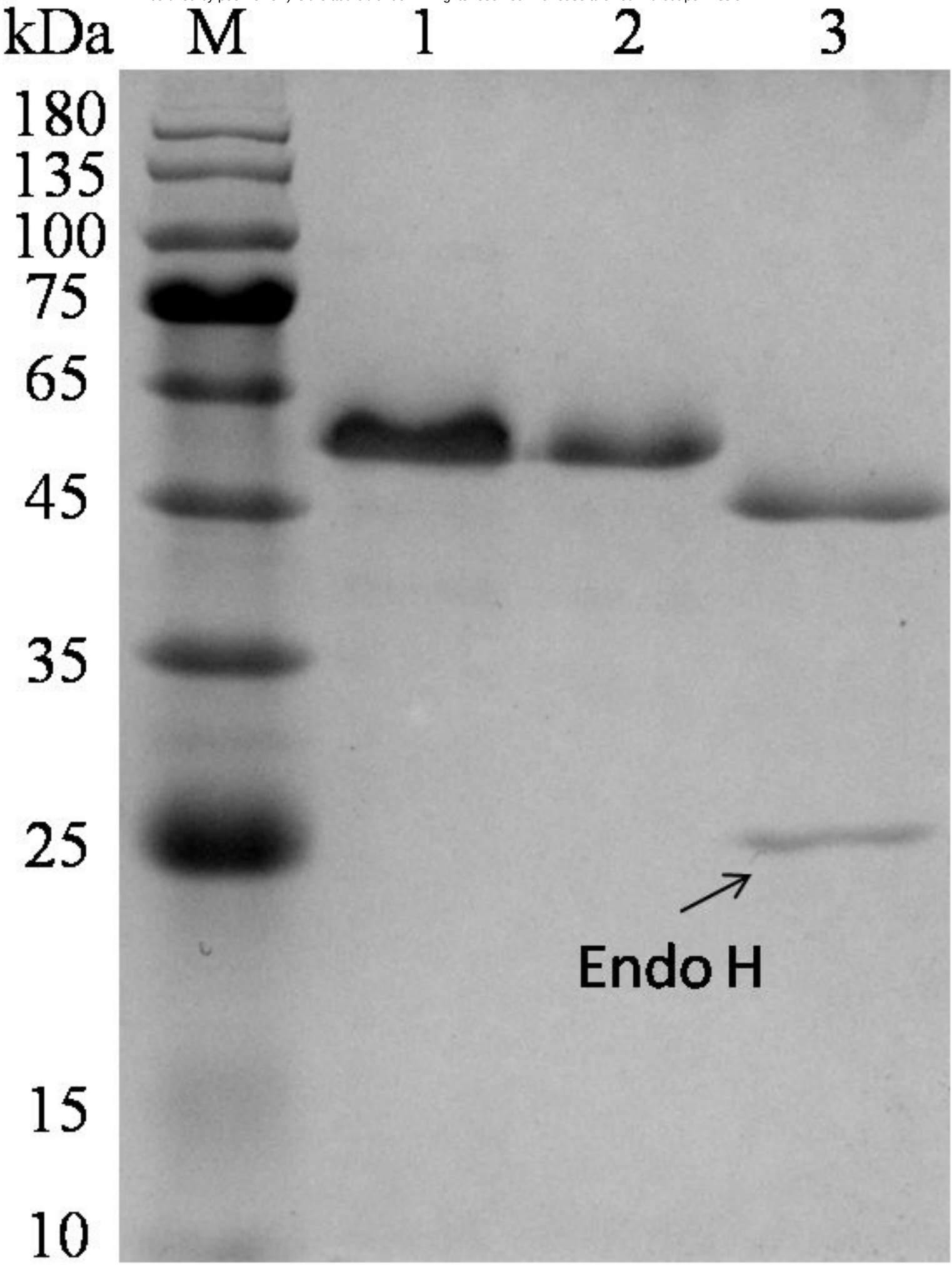

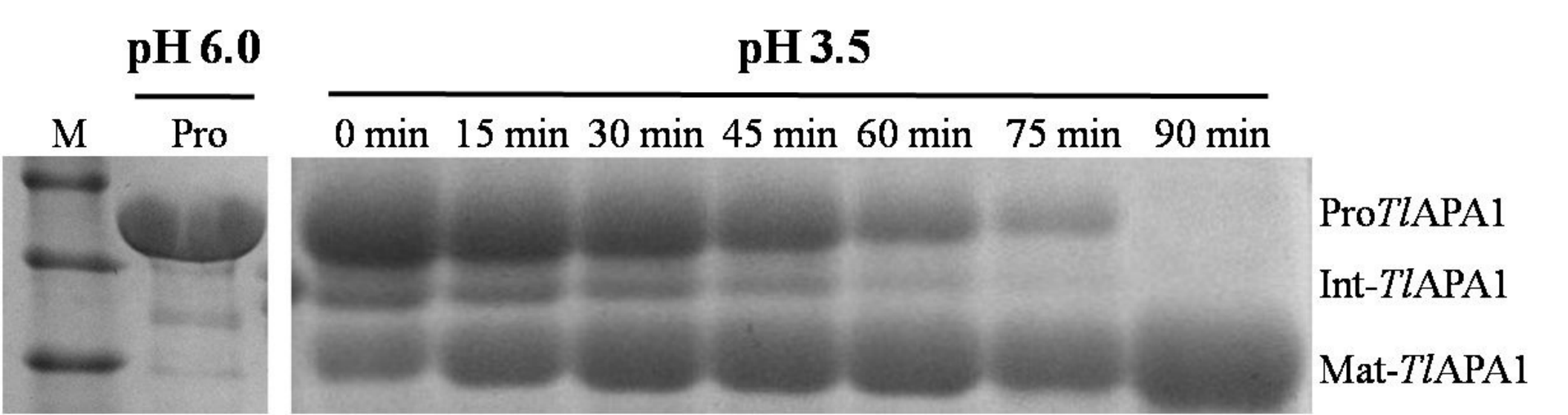
pH 6.0
pH 3.5
M
Pro
0 min
15 min
30 min
45 min
60 min
75 min
90 min
ProTlAPA1
Int-TlAPA1
Mat-TlAPA1

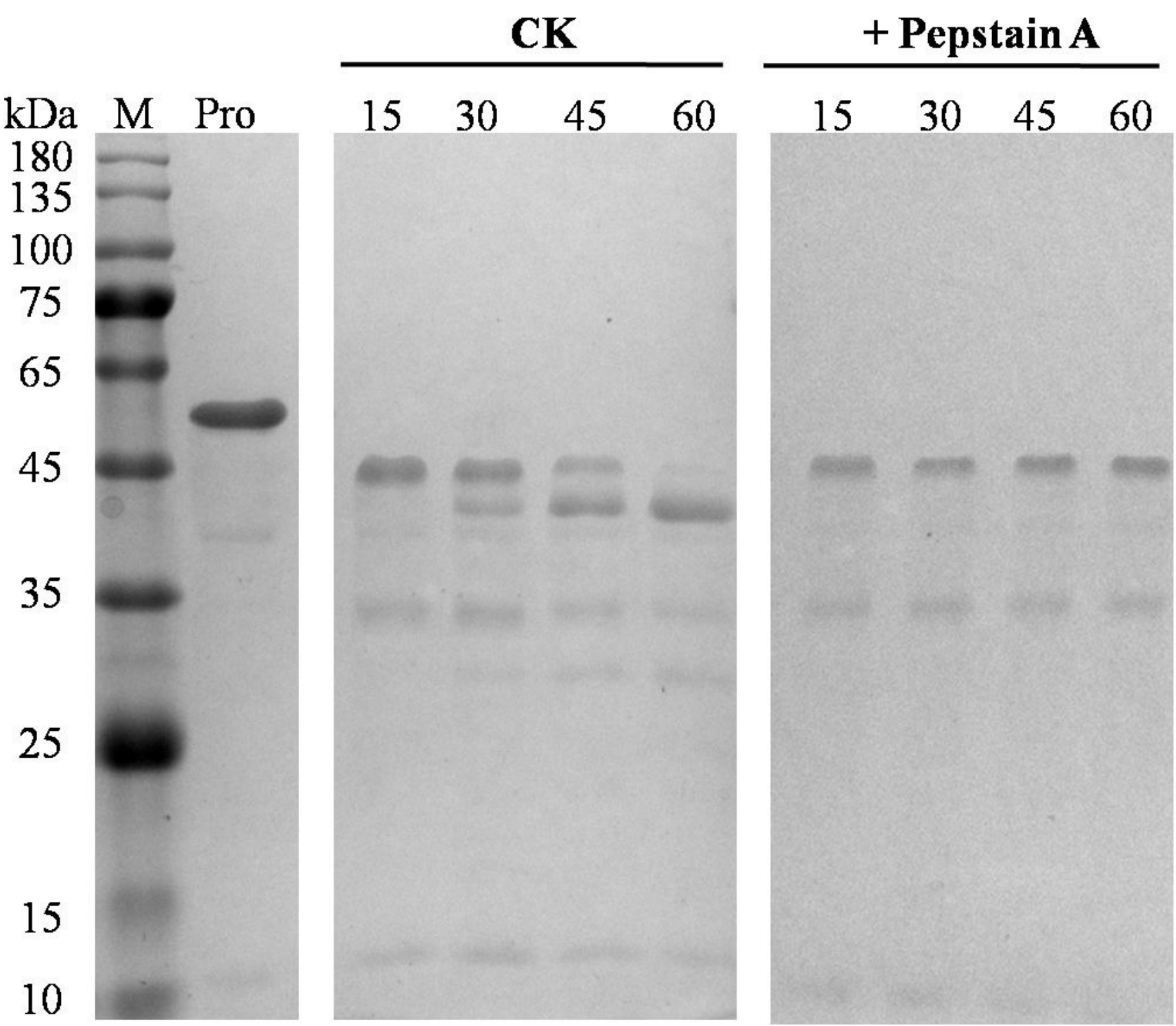
CK
+ Pepstain A
kDa
M
Pro
15
30
45
60
15
30
45
60
180
135
100
75
65
45
35
25
15
10

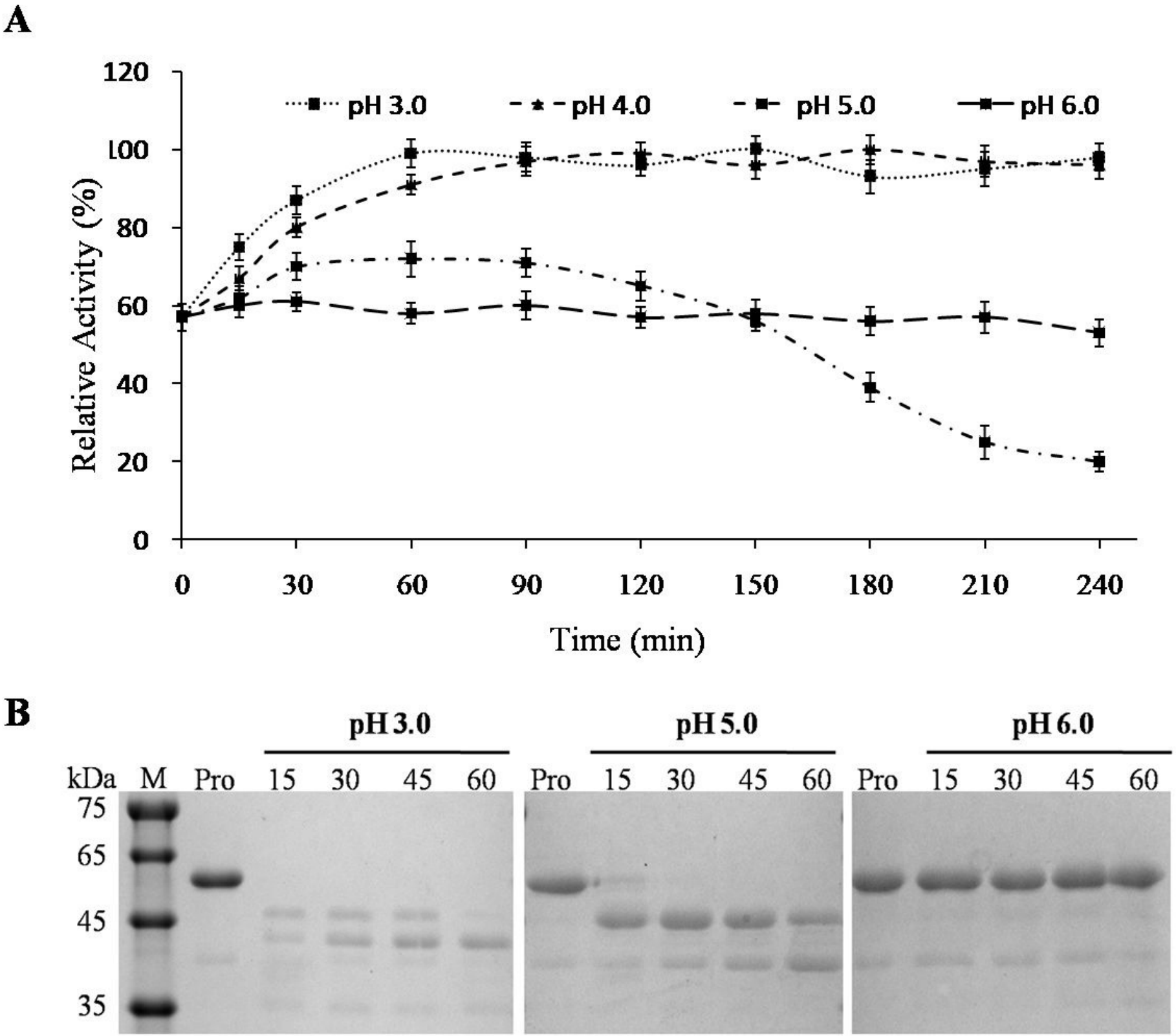
A
120
100
80
60
40
20
0
Relative Activity (%)
pH 3.0
pH 4.0
pH 5.0
pH 6.0
0
30
60
90
120
150
180
210
240
Time (min)
B
pH 3.0
pH 5.0
pH 6.0
kDa
M
Pro
15
30
45
60
75
65
45
35

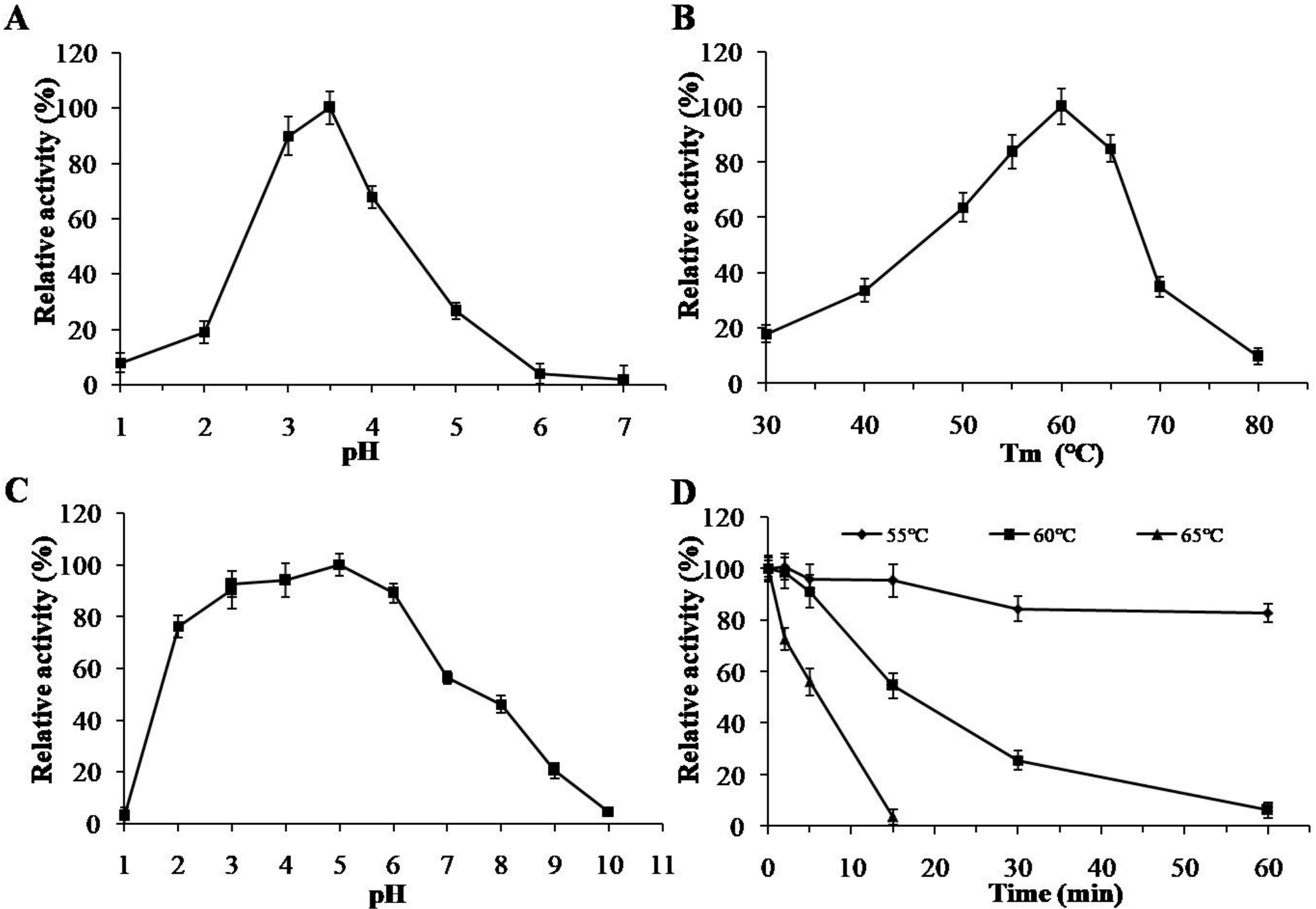
A
Relative activity (%)
120
100
80
60
40
20
0
1
2
3
4
5
6
7
pH
B
Relative activity (%)
120
100
80
60
40
20
0
30
40
50
60
70
80
Tm (℃)
C
Relative activity (%)
120
100
80
60
40
20
0
1
2
3
4
5
6
7
8
9
10
11
pH
D
55℃
60℃
65℃
Relative activity (%)
120
100
80
60
40
20
0
0
10
20
30
40
50
60
Time (min)

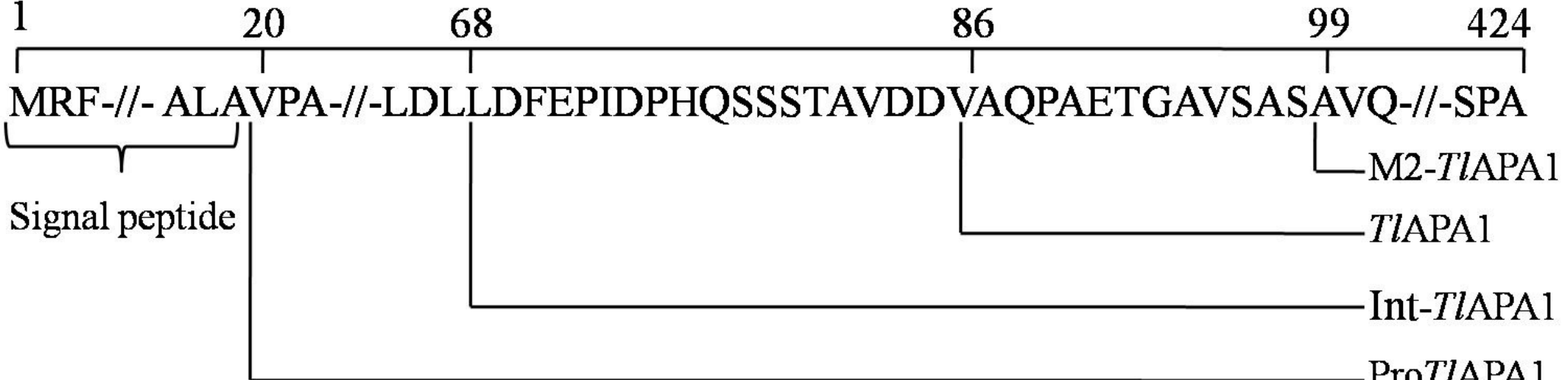
1
20
68
86
99
424
MRF-//- ALAVPA-//-LDLLDFEPIDPHQSSSTAVDDVAQPAETGAVSASAVQ-//-SPA
Signal peptide
M2-TlAPA1
TlAPA1
Int-TlAPA1
ProTlAPA1

Table 1 Primers used in this study.

Primers	**Sequences (5′→3′)**
*Tl*apa1F	GGGTACGTAGTCCCGGCTCCTTCGCGGCCT
*Tl*apa1R	GAGCCTAGGCTATGCAGGAGATGCAAAACCAAGAGATGGA

Table 2 Optimal temperature and thermostability of several aspartic proteases

Source	Products name	Optimal temperature (°C)	Thermostability (%)	Reference
T. leycettanus	*Tl*APA1	60	84% (55°C, 30 min)	This study
M. circinelloides	*MC*AP	60	40% (55°C, 30 min)	5
R. miehei	RmproA	55	60% (55°C, 30 min)	17
Aspergillus foetidus	*Af*AP	55	ND	13
T. asperellum	TAASP	40	ND	14
Cryptococcus sp.	Cap1	30	80% (50 °C, 60 min)	43
M. pilosus	MpiAP1	55	80% (55°C, 30 min)	42
A. repens	PepA_MK82	60	80% (50 °C, 20 min)	44

a. the values in the brackets indicate the incubation time at temperature (°C), and the percentages in front of the brackets indicate the residual activity.